Analytica Chimica Acta xxx (xxxx) xxx

Contents lists available at ScienceDirect

Analytica Chimica Acta

journal homepage: www.elsevier.com/locate/aca

A novel RNA aptamer-modified riboswitch as chemical sensor

Jing Wang [a, b, d, 1], Dongmei Yang [a, 1], Xiaogang Guo [c], Qitao Song [b], Luxi Tan [a, d, **], Lichun Dong [a, d, *]

[a] School of Chemistry and Chemical Engineering, Chongqing University, Chongqing, 400044, China
[b] College of Chemistry and Molecular Engineering, Peking University, Beijing, 100871, China
[c] Chongqing Key Laboratory of Inorganic Special Functional Materials, College of Chemistry and Chemical Engineering, Yangtze Normal University, Chongqing, 408100, China
[d] Key Laboratory of Low-grade Energy Utilization Technologies & Systems of the Ministry of Education, Chongqing University, Chongqing, 40004, PR China

HIGHLIGHTS

- The target would induce the conformational changes of RNA aptamer-modified *cis*-repressor sequences.
- The sensor can play its role to inhibit the expression of indicated gene without the target, and quickly responds to its target once the target arises.
- The sensitivity of the sensor has been significantly improved with fewer number of sequestered RBS sequences included in the crRNA.
- The developed sensor can fulfill the quantitative detection of the target chemical molecule *via* the GFP concentration encoded by the *gfp* gene.

GRAPHICAL ABSTRACT

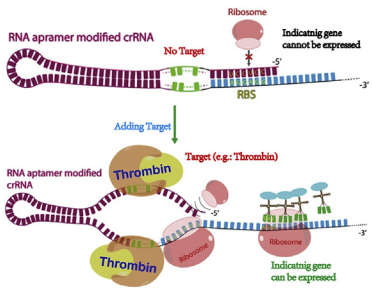

ARTICLE INFO

Article history:
Received 29 July 2019
Received in revised form
20 November 2019
Accepted 30 November 2019
Available online xxx

Keywords:
Sensor
RBS
Cis-repressor sequence
RNA aptamer
Riboswitch
Gene expression

ABSTRACT

In this study, a novel label- and immobilization-free RNA aptamer-modified riboswitch-based biosensor was developed by using RNA aptamer modified secondary-structural scaffolds to control the identity of the ribosomal binding sequence (RBS). In the developed sensor, the duplex RNA aptamers-modified *cis*-repressor sequence is introduced upstream to the RBS of the indicating gene (*gfp* gene), leading to formatting an RNA bubble due to the none-complementary state of the RNA aptamers in the hairpin structure of the *cis*-repressor sequence. Without the presence of the target molecule, the ribosome cannot identify the RBS of the indicating gene as the RBS is hidden by the introduced *cis*-repressor, consequently, the indicating gene in the sensor would not be expressed, demonstrating the absence of the target. On the contrary, with the presence of the target molecule, the binding of aptamer with the target would induce the enlargement of the RNA bubble, leading to the separation of the *cis*-repressor sequence and RBS. Hence, the indicating gene would be expressed, manifesting the existence of the target. In addition, the developed sensor can quantitatively report the target concentrations by measuring the *gfp* gene-encoded GFP (green fluorescent protein) concentration. The approach proposed in this study can be used to construct sensors for detecting various chemicals by introducing the

* Corresponding author. School of Chemistry and Chemical Engineering, Chongqing University, Chongqing, 400044, China.
** Corresponding author. 212, School of Chemistry and Chemical Engineering, Chongqing University, Chongqing, 400044, China.
E-mail addresses: tanluxi@cqu.edu.cn (L. Tan), lcdong72@cqu.edu.cn (L. Dong).
[1] Co-first Authors: Jing Wang and Dongmei Yang contributed equally to this work.

https://doi.org/10.1016/j.aca.2019.11.071
0003-2670/

corresponding aptamers, therefore, this strategy can potentially provide a new set of analytical tools in the field of analytical chemistry.

1. Introduction

Nucleic acid aptamer, including both RNA aptamer and DNA aptamer, can be screened against any interested ligands from a combinatorial library by using an iterative affinity selection procedure [1–3] at a relatively low cost [4,5]. Aptamers, often called as "chemical antibodies", are functionally comparable to the conventional antibodies [6], but offer a variety of advantages including the relatively flexible structure, small physical size, high stability, quick chemical production, versatile chemical modification and lack of immunogenicity [7–11]. On the other side, the predictive and rational design of nucleic acids can be facilitated with excellent chemical stability due to the current hybridization rules, meaning that aptamer can be used in the harsher environment with the characteristic of durability [12]. Therefore, aptamers can be used to substitute for antibodies as sensors to directly report analyte concentrations in heterogeneous assays [5,13]. Which are actively being sought in the literatures [14]. Currently, most of the developed aptamer-based sensors reply on the direct observation of the target-induced conformational changes as the unstructured aptamers form specific secondary structures upon binding with the target molecules such as three-way junctions like G-quadruplex structures [15–18]. Which are finding extensive applications in medical diagnostics, drug screening, environmental monitoring, etc [19,20].

However, the target-induced conformational changes are hard to control, such as, some aptamers for detecting target molecular have high dissociation constants [21], and some well-characterized aptamers for detecting target molecular are structurally stable and form a three-way junction even before binding with the target [15]. For improving the efficiency of the target-induced conformational changes, Stojanovic et al. reported to destabilize the RNA aptamer by truncating its sequences, so that the aptamer can exist in the equilibrium state which including both the unfolded structure and folded structure [22]. The destabilized aptamer exhibits the expected cocaine induced structure of folding, but still could form the folding structure in the absence of target, leading to a limited sensor sensitivity. This problem can be resolved by splitting the aptamer into two or three fragments, which significantly reduces the background signal; while the aptamer fragments can retain the capability to recognize the target by successfully reassembling into the complex secondary structure in the presence of cocaine. However, the splitting of aptamers significantly weakens the aptamer-target affinity; consequently, the sensitivity of the split aptamer-based sensor would be compromised.

Diverse cellular processes can be regulated by the noncoding RNAs, including the transcription and translation of gene expression [23]. Commonly, these functions are closely connected to t noncoding RNA's structure. An important such noncoding RNA element is the riboswitch, which typically locating in the 5′-untranslated region of prokaryotic protein coding transcripts [24]. Riboswitch is the region of mRNAs which contain specific evolutionarily conserved ligand-binding domain, termed the expression platform, that enables regulation of the downstream coding sequences of mRNA. The term "riboswitch" reflects the potential ability of these noncoding RNAs to function as biosensors [25]. In this study, we have successfully structured a novel label-and immobilization-free RNA aptamer-based sensor (G-EL sensor) based on the detection of the *gfp* gene expression, which was controlled by the exposure of ribosomal binding sequence (RBS) of mRNA *via* the target induced conformational changes of RNA aptamer-modified rioboswitch. It is well established that it is by the translation process that ribosomes read the genetic message in mRNA and produce amino acids product according to the instructions, which can be divided into three steps: initiation; elongation and termination. In the initiation phase, the ribosome binds to the RBS of mRNA, and the first amino acid, attached to its tRNA, also binds [26]. In addition, the small noncoding RNAs (sRNA) in prokaryotic provide the mechanism to precisely control of gene expression the translation, especially the regulatory RNA (riboregulator), which can control the expression of target genes to require a coordinated cellular response [27]. The *cis*-repressor (crRNA) included in the sRNA contains the sequence which complementary bind to the RBS, repressing the target gene expression by forming the hairpin structure upstream of RBS to prevent the ribosomal binding [28]. Herein, a duplex RNA aptamers-modified crRNA is introduced upstream to the RBS of *gfp* gene in the developed sensor, leading to forming an RNA bubble due to the none-complementary state of the RNA aptamer in the hairpin structure of crRNA. Without the presence of the target molecule, the *gfp* gene cannot be expressed as the RBS is hidden by the modified crRNA. While with the presence of the target, the RNA bubble would be enlarged around the duplex aptamers in the local structure of crRNA due to the binding of aptamers with the target (Fig. 1a–b); consequently, the RBS in the RNA bubble can be recognized and bound by ribosome, which leads to the expression of the target gene. As the more concentration of target in the detection system, proportional number of RBS can be recognized, leading to expressing the proportional concentration of green fluorescent protein (GFP) encoded by *gfp* gene, the concentration of the GFP can be measured to quantify the concentration target ((y-n)/m; y: the GFP concentration; n: the GFP concentration for the sample without target, in this study n is 0 at the optimal conditions; m: the ratio between increasing concentration of GFP and the increasing concentration of target). When the concentration of target is enough for enlarged the certain number RNA bubble, the GFP concentration encoded by *gfp* gene reached to highest (a), hence, the target concentration should be diluted to less than c (c: the largest concentration of target which G-EL sensor can quantify) for quantifying (Fig. 1c).

2. Experimental

The methods can be seen in the Supporting Information (Construction of plasmids; mRNA analysis). Primers, plasmids used in this study can be seen in Table S1. Structure sequences of the six *cis*-repressor elements were constructed according to our previous study [29], in the dark blue circle is the start code sequence (AUG); in the red circle is the RBS sequence (AGGAGG) (Fig. S1). Structure sequences of the three duplex thrombin RNA aptamers modified crRNA 2 with different distance between the downstream RNA aptamer and ribosome (DBDRAR: 11 bp, 6 bp and 16 bp), the green sequences are the thrombin RNA sequences, in the dark blue circle is the start code sequence (AUG); in the red circle is the RBS

Please cite this article as: J. Wang et al., A novel RNA aptamer-modified riboswitch as chemical sensor, Analytica Chimica Acta, https://doi.org/10.1016/j.aca.2019.11.071

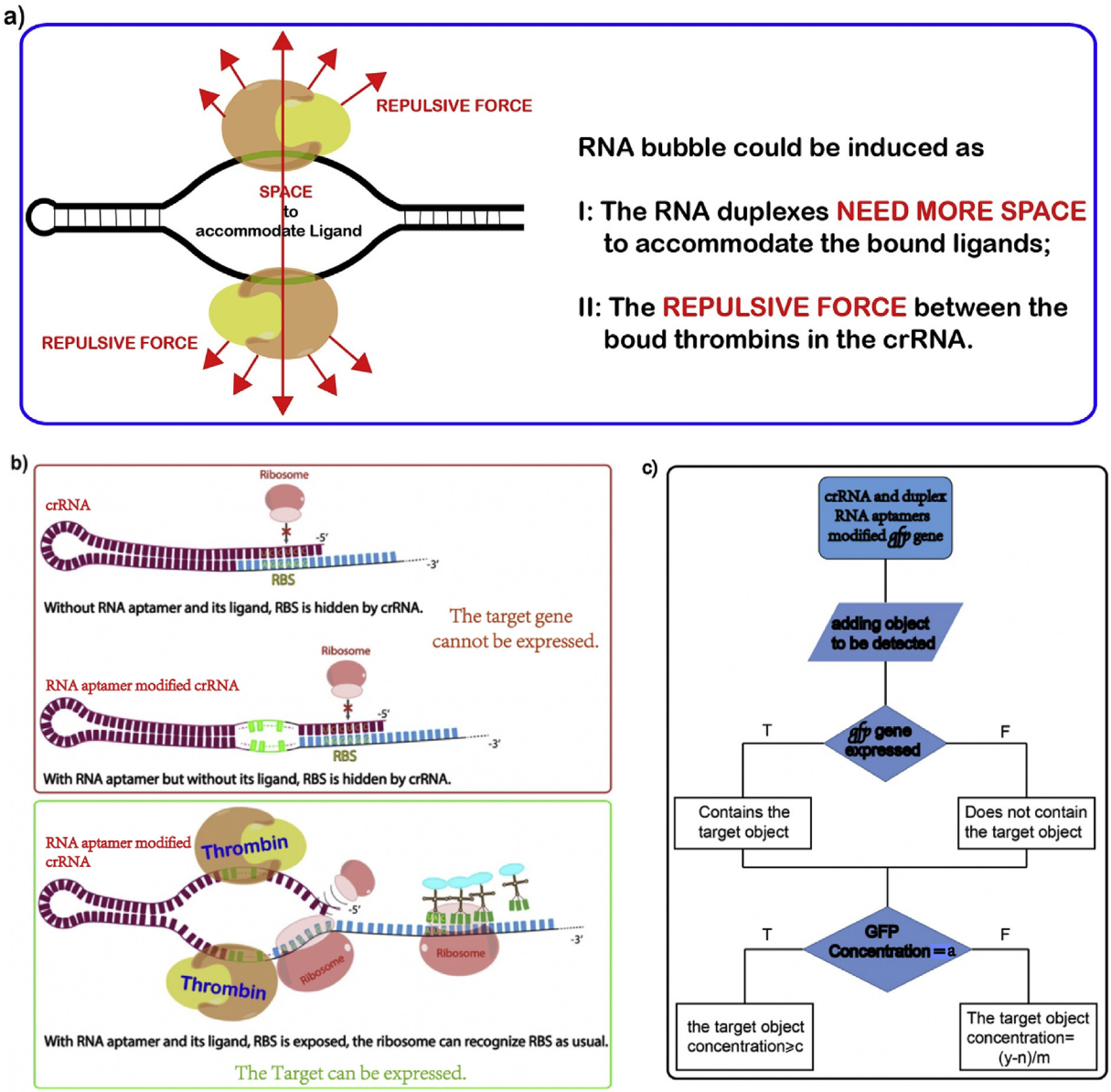

Fig. 1. The working mechanism of the developed G-EL sensor. (a) The formation and enlargement of the RNA bubble. (b) Without the presence of the target, the indicating gene (*gfp* gene in this study) in the sensor would not be expressed since the ribosome cannot identify the ribosomal binding sequence (RBS) of the indicating gene due to the hiding of the RBS *via* the introduced *cis*-repressor sequence complementing to the RBS, manifesting the absence of the target; with the presence of target, the RNA bubble would be enlarged around the duplex aptamers in the local structure of crRNA due to the binding of aptamers with target; consequently, the RBS in the RNA bubble can be recognized and bound by ribosome, leading to the expression of the indicating gene, indicating the existence of the target. (c) The working mechanism of the sensor to quantitatively calculate the target concentration.

sequence (AGGAGG) (Fig. 2). Structure sequences of the five duplex thrombin RNA aptamers modified crRNA with DBDRAR = 11 bp, in which, the modified crRNA naturally folds to a structure that sequesters the different numbers of RBS sequences, preventing the translation of downstream genes. The green sequences are the thrombin RNA sequences, in the dark blue circle is the start code sequence (AUG); in the red circle is the RBS sequence (AGGAGG), the black circle is the sequestered sequences of RBS (Fig. S2). Structure sequences of the five duplex different RNA aptamers modified crRNA 2–1 with DBDRAR = 11 bp, the green sequences are the RNA sequences, in the dark blue circle is the start code sequence (AUG); in the red circle is the RBS sequence (AGGAGG), the black circle is the sequestered sequences of RBS (Fig. S3). The 7 fragments of the modified or none modified *gfp* genes were obtained through the method of PCR (Fig. S4-Fig. S10).

Calibration experiment of the G-EL sensor. Firstly, the S30 premix and the cell extract from the Promega S30 T7 High-Yield Expression System kit (Promega TM306) were mixed in the proportion recommended by manufacturer (reaction buffer), and added the GFP (bs-0890P, bioss, China) to the final concentration of 0, 0.2 μM, 0.4 μM, 0.6 μM, 0.8 μM, 1.0 μM, 1.2 μM, 1.4 μM, 1.6 μM 1.8 μM and 2.0 μM, respectively in 1 mL. Fluorescence measurements (485/20 nm excitation, 528/20 nm emission) were made in a Biotek Synergy 2 plate reader, and then obtaining the standard curve between the GFP concentration and fluorescence intensity. The Promega S30 T7 High-Yield Expression System kit was used for Cell-Free Protein Synthesis experiments (GFP in this study). The G-EL sensor were used at 25 ng/μL concentration per reaction in the reaction buffer, the thrombin or VEGF was added to the final concentration of 0, 0.2 μM, 0.4 μM, 0.6 μM, 0.8 μM, 1.0 μM, 1.2 μM,

Please cite this article as: J. Wang et al., A novel RNA aptamer-modified riboswitch as chemical sensor, Analytica Chimica Acta, https://doi.org/10.1016/j.aca.2019.11.071

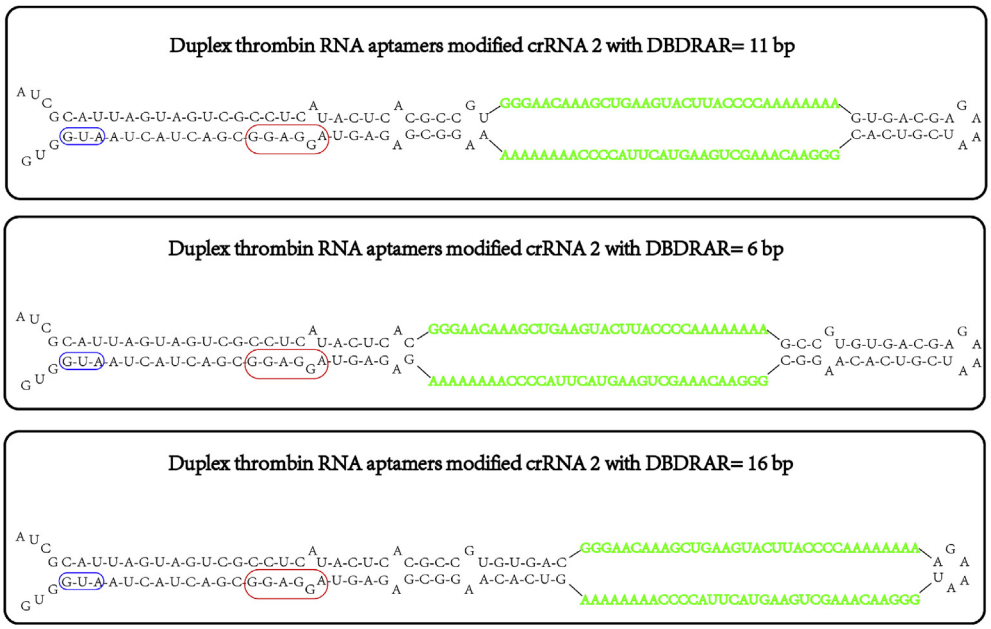

Fig. 2. Structure sequences of the three duplex thrombin RNA aptamers modified crRNA 2 with different DBDRARs (11 bp, 6 bp and 16 bp), in which, the modified crRNA is within the 5′-untranslated region of the mRNA and naturally folds to a structure that sequesters the whole RBS sequences, preventing the translation of downstream genes. The green sequences are the thrombin RNA sequences, in the dark blue circle is the start code sequence (AUG); in the red circle is the RBS sequence (AGGAGG). (For interpretation of the references to colour in this figure legend, the reader is referred to the Web version of this article.)

1.4 μM, 1.6 μM 1.8 μM—5.0 μM, respectively per reaction, all the reactions were set up in Corning CLS3820 plates following manufacturer's instructions. For the GFP assays, the synthesis reactions of cell-free proteins were prepared firstly, incubated at 30 °C with shaking for 6 h, and fluorescence measurements (485/20 nm excitation, 528/20 nm emission) were made every 7 min in a Biotek Synergy 2 plate reader. Values indicated in the graphs representing GFP concentrations were obtained after 6 h of synthesis reactions, then obtaining the calibration curve between the target (thrombin and VEGF in this study) and GFP concentration. The used thrombin (MP Biomedicals, USA) and VEGF (bs-0279R, bioss, China) were prepared by diluting the stock solution (in 50% glycerol) into 10 mM Tris-HCl pH 7.5 and 50 mM KCl to ensure that the final glycerol concentration in the cell-free protein synthesis reactions is less than 0.5%.

Detection limit experiments for the G-EL sensor. 3 solutions without of target were added to the reaction buffer with 25 ng/μL G-EL sensor, incubated at 30 °C with shaking for 6 h, and fluorescence measurements (485/20 nm excitation, 528/20 nm emission) were made for the 3 solutions, we report the average of 5 fluorescence signals emerging from the fluorescence detector without adding the target. After having obtained the SD of blank signal, this value has been multiplied three times and use this value in the formula obtained from the calibration curve to extrapolate the value of target concentration corresponding to the detection limit of the G-EL sensor.

The authors should report the average and SD of >3 fluorescence signals emerging from the fluorescence detector without adding the target (black). I can understand that the signal could be near zero but it is difficult to believe that any background signal is produced by the solution. After having obtained the SD of blank signal, this should be multiplied three times and use this value in the formula obtained from the calibration curve in order to extrapolate the value of target concentration corresponding to the LOD.

Thrombin detection in human serum. G-EL sensor for thrombin detection: the Promega S30 T7 High-Yield Expression System kit was used for Cell-Free Protein Synthesis experiments (GFP in this study). The G-EL sensor were used at 25 ng/μL concentration per reaction in the reaction buffer and the diluted human serum with thrombin was added, incubated at 30 °C with shaking for 6 h, and fluorescence measurements (485/20 nm excitation, 528/20 nm emission) were made, the thrombin concentration was calculated by the calibration curve between the target and GFP concentration. ELISA for thrombin detection: Thrombin-antithrombin (TAT) complexes formed following the neutralization of thrombin by antithrombin III have been used as a surrogate marker for thrombin detection. TAT complexes were examined by ELISA with the Thrombin- Antithrombin Complex Human ELISA Kit (ac108907, Abcam). Briefly, diluted human serum with thrombin was added into each well of a microtiter plate and incubated for 2 h. Each well was washed and 50 μl of 1 × Biotinylated Thrombin-Antithrombin Complex antibody was added, followed by incubation for 1 h. Then the well was washed and 50 μl of 1 × SP conjugate was added. After 30 min, the well was washed and 50 μl of chromogen substrate was added. The reaction was stopped after 30 min. The plates were read at 450 nm with a Variskan Flash Spectral Scanning Multimode Reader (Thermo Scientific).

3. Results and discussion

3.1. Effectiveness of the G-EL sensor

The following six sequences with different thermodynamic stability (crRNA1, crRNA2, crRNA3, crRNA4, crRNA5 and crRNA6) were selected to repress the translation of the target mRNA (Fig. S1). According to the Zuker's method [30], the ΔG value for the six *cis*-repressor element are: crRNA 1, -41.4 kcal·mol-1; crRNA2, -60.4 kcal·mol-1; crRNA3, -45.6 kcal·mol-1; crRNA4, -47.5 kcal·mol-1; crRNA5, -49.9 kcal·mol-1; crRNA6, -56.3 kcal·mol-1, respectively. The inhibitory effect of the crRNAs for translating target mRNA was determined by measuring the GFP concentration. As shown in Fig. 3a, the GFP concentration of

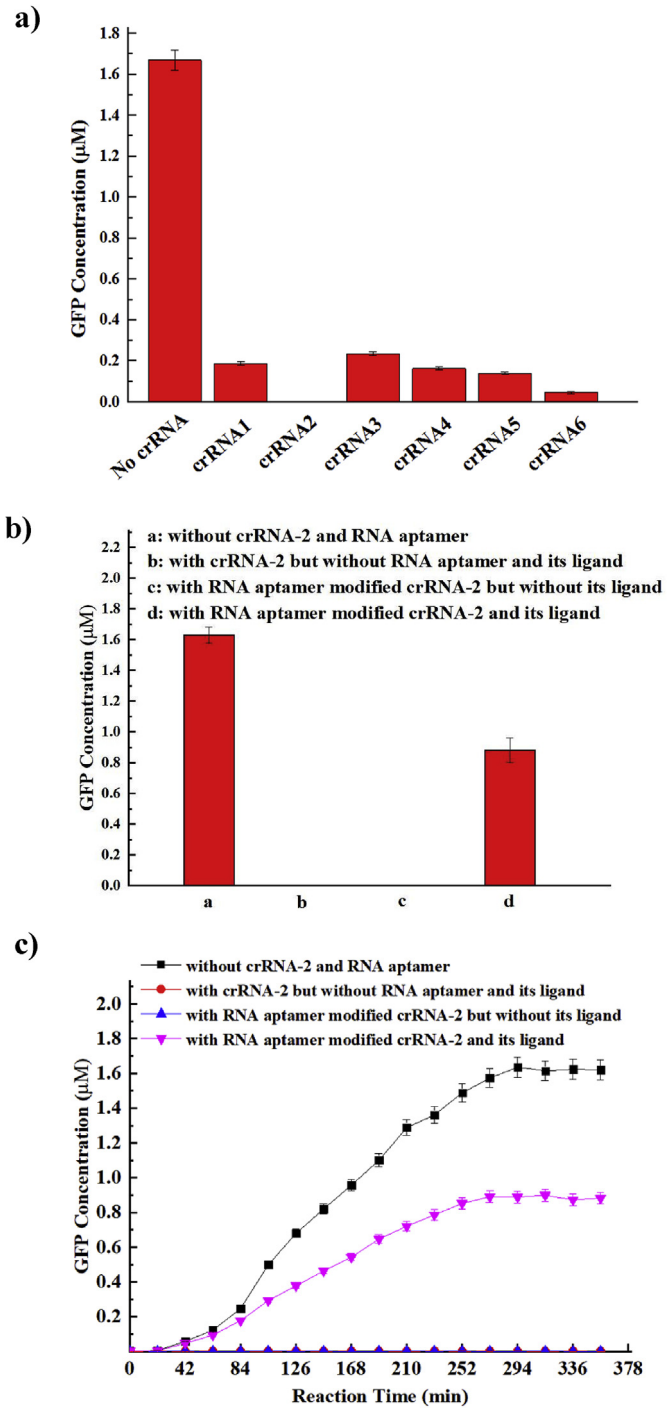

Fig. 3. Effect of the inhibited element (crRNA) and activated element (RNA aptamer modified crRNA with its target) of the G-EL sensor on the GFP concentration (DBDRAR = 11 bp). (a) GFP concentration of templates introduced with different crRNAs after 6 h of cell-free protein synthesis experiments without of thrombin. (b) GFP concentration of templates introduced with crRNA 2 or RNA modified crRNA 2 after 6 h of cell-free protein synthesis experiments with/without the existence of 2.6 μM thrombin. (b) Kinetics of GFP concentration of templates introduced with crRNA 2 or RNA modified crRNA 2 after 6 h of cell-free protein synthesis experiments with/without the existence of 2.6 μM thrombin.

templates with crRNA exhibited a significant decrease compared to that of the template without crRNA. Moreover, the *gfp* gene expression becomes weaker with the increased thermodynamic stability of the *cis*-repressor elements. The typical case is that the *gfp* gene expression in the template harboring crRNA2 was completely inhibited (no GFP concentration was detected), while the expression level in the template harboring crRNA3 was significantly high (the GFP concentration was 0.24 μM). Therefore, crRNA2 modified by the duplex thrombin RNA aptamers with the distance between the downstream RNA aptamers and the RBS (DBDRAR) of 11 bp was chosen to construct the sensors for detecting thrombin. At the situation without thrombin, the GFP concentration of the template introduced with the modified crRNA2 exhibited no obvious difference compared with that of the template introduced with the original crRNA2 (Fig. 3b–c) as the *gfp* gene expression was completely inhibited in both templates, demonstrating that the developed sensor can indicate the absence of thrombin by the non-expression of the *gfp* gene. On contrary, in the presence of thrombin of 2.6 μM, the *gfp* gene expression of the template introduced with the modified crRNA2 can be turned to the "ON" state (the corresponding GFP concentration was 0.89 μM), while the *gfp* gene for the template introduced with the original crRNA2 was still not be expressed, clarifying that the developed sensor can manifest the existence of thrombin by switching the *gfp* gene expression to the "ON" state.

3.2. Effect of the distance between the downstream RNA aptamers and the RBS on the G-EL sensor

The performance of the developed thrombin sensors introduced with the modified crRNA2 of different DBDRARs (6 bp, 16 bp) was compared in Fig. 2, showing that although the *gfp* gene in both sensors can be expressed with the presence of thrombin (2.6 μM), the GFP concentration for the template introduced with the modified crRNA2 of DBDRAR = 6 bp was only 0.19 μM (Fig. 4), much lower than that for the template introduced with the modified crRNA2 of DBDRAR = 16 bp (0.48 μM), indicating a lower sensitivity of the sensor with DBDRAR = 6 bp at the aspect of display intensity level. The dependence of the sensor's sensitivity on distance between the RBS site and the duplex RNA aptamers can be classified into the followed four scenarios: i) the RBS cannot be contained in the induced RNA bubble when the distance between the RBS site and the duplex RNA aptamers is too long (Fig. 5a); the *gfp* gene cannot be expressed even with the presence of thrombin, the sensor loses the ability to detect the target; ii) when the RBS are contained in the induced RNA bubble but in the edge, ribosome can partially regain the recognition ability to the RBS, the *gfp* gene can be expressed at a low level (Fig. 5a), resulting in the low sensitivity of the sensor; iii) when the RBS site is contained in the middle region of the induced RNA bubble at a suitable range of DBDRAR, the ribosome can recognize the RBS site with the presence of thrombin, leading to the maximum expression of the *gfp* gene under crRNA (Fig. 5a), representing the best sensitivity of the corresponding sensors; iv) when DBDRAR is too short, although the RBS can be contained in the induced RNA bubble, the RBS site could be sequestered by the bound target, resulting in the weakened recognition of the RBS by ribosome (Fig. 5a), the sensitivity of the corresponding sensors is poor due to the low *gfp* gene expression. Fig. 5b demonstrated the different concentrations of GFP for the templates with different DBDRARs in the presence of 2.6 μM thrombin. No RBS sequence can be contained in the induced RNA bubble when DBDRAR >23 bp, the induced RNA bubble could not affect the expression of the *gfp* gene, resulting in the silence of the *gfp* gene (GFP concentration was 0). When 11 bp < DBDRAR<23 bp, the increased GFP concentration could be obtained with the decreased DBDRAR, indicating that the sensor's sensitivity based on the *gfp* gene expression can be enhanced by decreasing DBDRAR. At this case, the induced RNA bubble starts to contain the RBS sequences when the DBDRAR = 23 bp. The improved recognition of

Please cite this article as: J. Wang et al., A novel RNA aptamer-modified riboswitch as chemical sensor, Analytica Chimica Acta, https://doi.org/10.1016/j.aca.2019.11.071

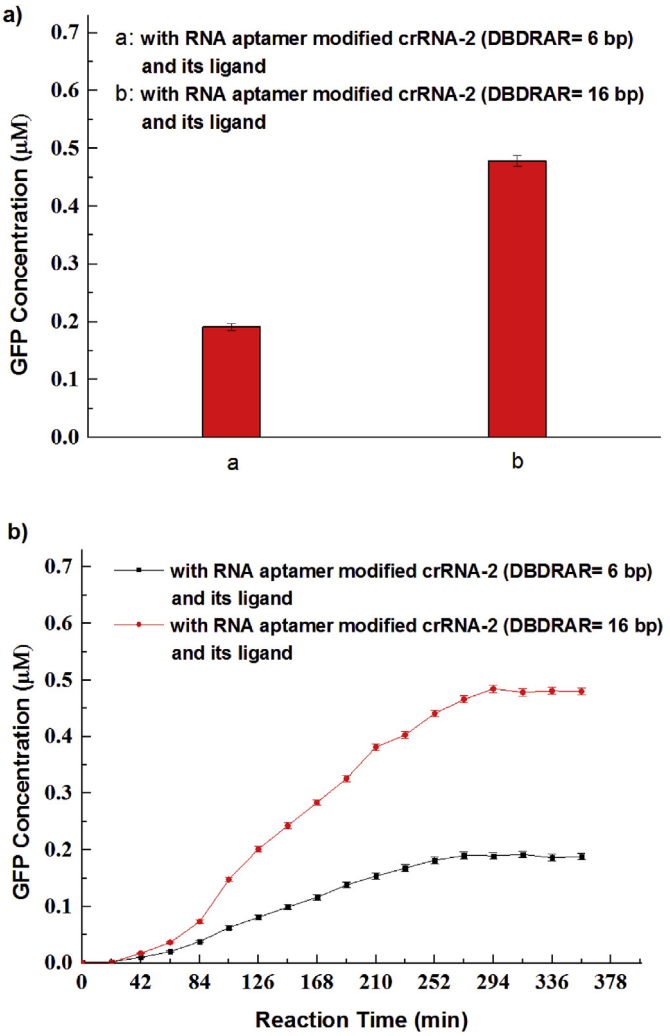

Fig. 4. Effect of different DBDRARs (6 bp and 16 bp) of G-EL sensor on the GFP concentration. (a) GFP concentration of templates introduced with different DBDRARs (6 bp and 16 bp) after 6 h reaction of cell-free protein synthesis experiments with the existence of 2.6 μM thrombin. (b) Kinetics of GFP concentration of templates introduced with different DBDRARs (6 bp and 16 bp) after 6 h reaction of cell-free protein synthesis experiments with the existence of 2.6 μM thrombin.

ribosome to the RBS at a smaller DBDRAR leads to significantly enhancement of the proposed sensor's sensitivity. While when DBDRAR <11 bp, the bound thrombin starts to sequester the RBS site; the expression of *gfp* gene decreases sharply with a decreased DBDRAR. Finally, when DBDRAR is decreased to 6 bp, the bound thrombin sequesters the RBS site completely, the expression of *gfp* gene reaches the lowest level. Therefore, the optimum DBDRAR for the developed thrombin sensor is 11 bp.

3.3. Effect of the sequestered RBS number by the RNA aptamer modified cis-repressor on the G-EL sensor

The sensitivity of a detection sensor can be usually reflected by two indicators: the "display intensity level" and "detection efficiency". For the conventional aptamer-based sensors that detect the target *via* the direct observation of the target-induced conformational changes [15–18], the "display intensity level" can be characterized by the amounts of aptamers with the conformational change; while for the developed G-EL sensor, the "display intensity level" can be measured by the GFP concentration. The other indicator of "detection efficiency" represents the detecting speed of the sensors with the aim to pursuer rapid, or even real-time detection [31]. For further improving the developed sensor's sensitivity in the aspect of "detection efficiency", five crRNAs with the same ΔG value (−60 kcal mol^{-1}) of crRNA2 (crRNA2-1, crRNA2-2, crRNA2-3, crRNA2-4, crRNA2-5) but with the different sequestered numbers of RBS sequence (NSRBS = 1 to 5) were designed and compared with the crRNA2 sequestering the whole RBS sequences (NSRBS = 6). The five crRNAs (DTMcrRNA2-1, DTMcrRNA2-2, DTMcrRNA2-3, DTMcrRNA2-4, DTMcrRNA2-5) modified by duplex thrombin RNA aptamers (DBDRAR = 11bp) (Fig. S2) were encoded upstream of the *gfp* gene, respectively. The results in Fig. 6 indicated that the "detection efficiency" of the constructed sensors increases with a decrease in NSRBS; the template with DTMcrRNA2-1 (NSRBS = 1) displayed the fastest speed to reach the maximum GFP concentration, while the template with DTMcrRNA2-5 (NSRBS = 5) was the slowest to reach the maximum GFP concentration. It is reasonable that the RBS with fewer number of sequestered sequences included in the crRNA can be activated more promptly by the enlarged RNA bubble.

3.4. Verification of the G-EL sensor by detecting VEGF

Fig. 7a demonstrated the calibration curve of GFP concentration *versus* thrombin concentration for the optimized sensor (sensor modified with DTMcrRNA2-1 and DBDRAR = 11bp) over a range of 0.2 μM–3.8 μM. Without thrombin, the *gfp* gene cannot be expressed, indicated by the zero GFP concentration. After thrombin are added, the GFP concentration firstly increases linearly with an increase in thrombin concentration until it reaches the value of 3.8 μM, then keeps constant with a further increase in thrombin concentration due to the saturation of RNA aptamers by thrombin. Moreover, it was demonstrated that the detection limit of thrombin is 88 nM. By following the same strategy, the sensors for detecting VEGF can also be constructed by introducing the corresponding duplex RNA aptamers in the DTMcrRNA2-1 (Fig. S3). Fig. 7 verified that similar results can be obtained for all the constructed sensors, but the maximum GFP concentration, the detection range and limit for the different sensors are distinct (for VEGF, the detection range is 0.2 μM–3.0 μM, and the detection limit is 55 nM). The reasons can be explained in two aspects: i). The affinity between different RNA aptamers and their specific ligands is different, leading to the different amounts of the target-bound aptamers [32,33]; ii). The size of the introduced RNA bubbles is different due to the varied molecular weight of target and target-aptamer binding force [34]. In Table 1, the developed sensor was compared with other nucleic acid-based sensors reported in the literatures [35–38]; in most cases, the immobilization-free sensors have the shortcoming of lower sensitivity compared to their immobilization-based sensors without any signal amplification, which is one of the important reasons that the development of the immobilization-free approaches was restricted. Xiang et al. [35] reported a label-free sensor for detecting thrombin based on the ultrasensitive electrochemical-based measurement for a G-rich secondary aptamer with PCR amplification, which is highly sensitive in the range from 27 fM to 2.7 nM. However, the strategy still requires the immobilization of DNA probe. On the contrary, the sensor developed in this study is label-free and immobilization-free, simple, low cost, and robust, which could potentially provide a new set of analytical tools for clinical chemistry.

Gene expression including two steps (transcriptional or the translational) [39]; while if the transcription level of the gene expression is affected by the introduced RNA bubble, the amount of the GFP concentration would also be affected [40]. Therefore, the mechanism for the developed sensor should be further proofed,

Please cite this article as: J. Wang et al., A novel RNA aptamer-modified riboswitch as chemical sensor, Analytica Chimica Acta, https://doi.org/10.1016/j.aca.2019.11.071

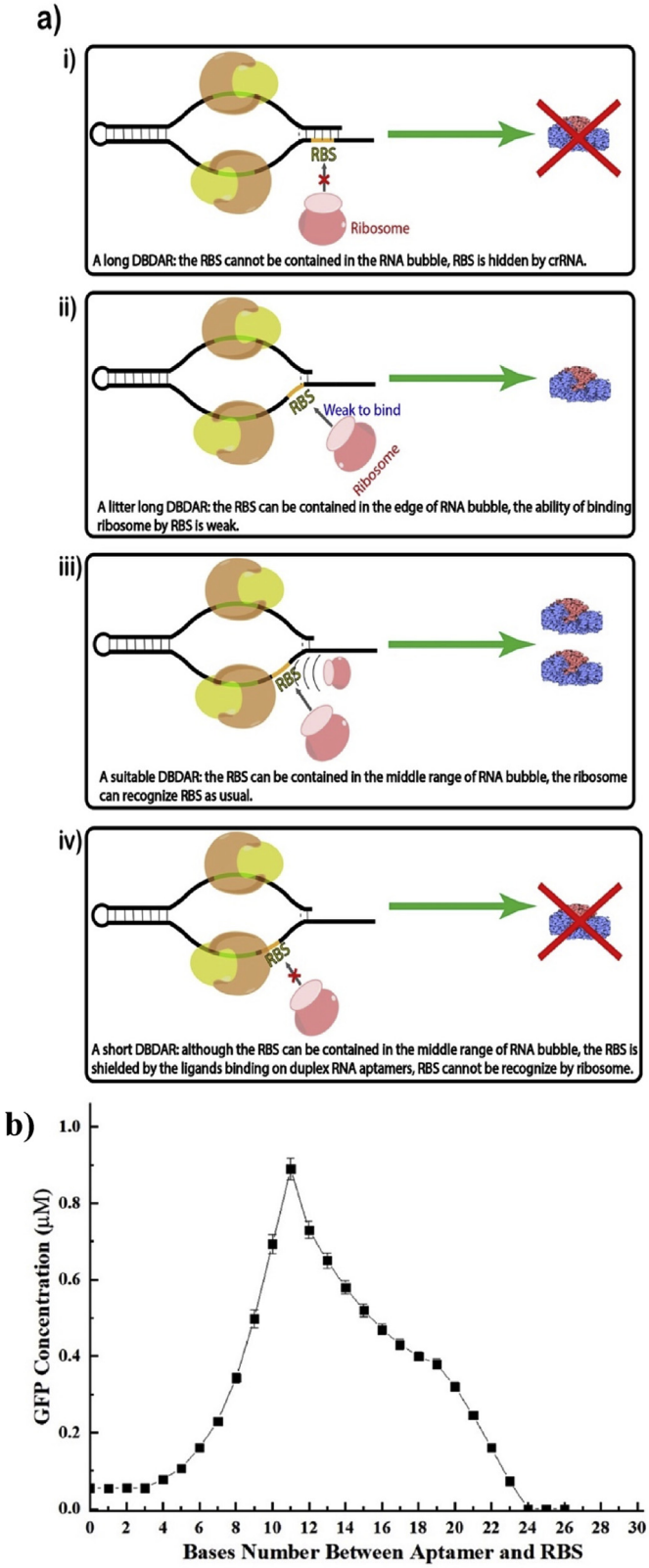

Fig. 5. Effect of different distances between RNA aptamer and RBS on G-EL sensor's sensitivity at the "display intensity level". (a) i) when the distance is too long, the RBS sequences cannot be contained in the induced RNA bubble, whose enlargement would not affect the *gfp* gene expression, the G-EL sensor loses the function for detecting the target; ii) when the RBS sequences is contained in the edge of the induced RNA bubble, the recognition capability of ribosome to the RBS can be re-activated to some extent by the enlarged RNA bubble; consequently, the *gfp* gene can be expressed at a low level, the sensitivity of the sensor is poor; iii) when the RBS sequences are contained in the middle region of the induced RNA bubble at a suitable range of DBDAR, the recognition of ribosome to the RBS can be re-activated completely, leading to the maximum expression of the *gfp* gene under crRNA, the sensitivity of the sensor is high; iv) when DBDRAR is too short, although the RBS sequences can be contained in the DNA bubble, the recognition region of the RBS is presumably sequestered by the bound target, resulting in the weakened recognition of the RBS by ribosome and low expression of the *gfp* gene, the sensitivity of sensor is poor. (b) GFP concentration of the template introduced with RNA aptamer modified crRNA2 under different DNDRARs after 6 h of cell-free protein synthesis experiments with the existence of 2.6 μM thrombin.

accordingly, the proposed sensor was investigated under the different concentrations of ligands, in which, the *gfp* gene expression was evaluated by analyzing mRNA using the real-time quantitative PCR at the transcription level and by testing the GFP concentration at the translation level. As showed in Fig. 7b, with the different concentrations of target (thrombin in this study), the multiple of *gfp* mRNA amplification is constant, whereas the GFP concentrations are almost proportional to the ligand concentration, confining that the developed sensors detect the target by analyzing the *gfp* gene expression at the translation level.

3.5. Thrombin detected in human serum

Human serum, which is considered as one of the most complex sample matrices, was imported in the detection system to test the stability of the established array technology. To access the applicability of the assay in complex biological samples, diluted human serum without thrombin was used as a sample matrix to evaluate the recovery in the assay. The added thrombin (0.2 μM, 1.0 μM, 1.5 μM, 2.0 μM, 3.0 μM) in the 100-fold diluted human serum with 10 μl per sample was detected by our G-EL sensor and the ELISA assay, respectively. The results are presented in Table 2. The recovery values of the added thrombin detected by GE-sensor were 89%–117% with relative standard deviations (RED) below 10%, similar with the recovery values of the added thrombin detected by ELISA (93%–107% with relative standard RED below 5%). It proved the feasibility of this establishing platform and indicated that the method has potential for quantitative detection of thrombin and design of a clinic diagnostic kit in biological samples.

4. Conclusions

In summary, we have developed a strategy for engineering label-free, immobilization-free, G-EL sensors *via* the crRNA and RNA aptamer-controlled *gfp* gene expression, which are accurate and can be used for detecting any chemicals whose binding aptamers can be found or synthesized. Without the target, the *gfp* gene expression in the sensor is inhibited by the RNA aptamer modified crRNA as the RBS is hidden by the modified crRNA; while at the presence of the target, the binding of the target with the RNA aptamer included in the crRNA would induce the enlargement of the RNA bubble, which leads to the exposure of the RBS sequences and the subsequent recognition and binding by ribosome. Consequently, the *gfp* gene can be expressed, manifesting the presence of the target. More significantly, the G-EL sensor can quantitatively report the target concentrations by measuring the *gfp* gene-encoded GFP concentration. The developed G-EL sensors are not dependent on the direct observation of the target-induced conformational changes of RNA aptamer, which are the commonly-used approach in the current aptamer-based chemical sensors. Recently, Stojanovic and Landry [22] have reported a detecting strategy by analyzing the changes in fluorescence, resulting in the double-end labeled (a fluorophore and a quencher) aptamers; therefore, the operation of the developed sensor is also based on the indirect monitoring of the aptamer-based

Please cite this article as: J. Wang et al., A novel RNA aptamer-modified riboswitch as chemical sensor, Analytica Chimica Acta, https://doi.org/10.1016/j.aca.2019.11.071

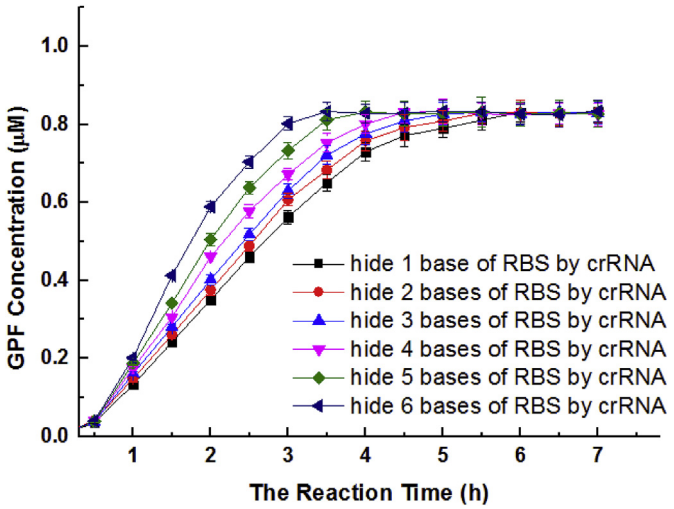

Fig. 6. Kinetics of GFP concentration for templates introduced with crRNA2 modified by the thrombin RNA aptamers (DBDRAR = 11 bp) under different numbers of sequestered RBS sequences.

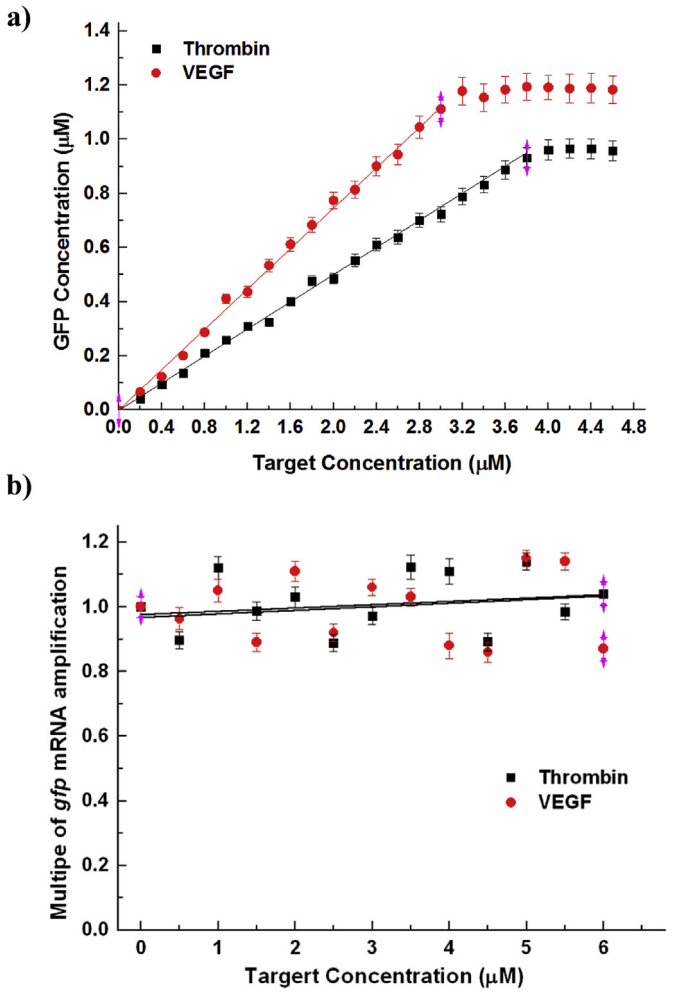

Fig. 7. (a) Calibration curves of the G-EL sensors for detecting different targets. (b) Effect of the G-EL sensors on the *gfp* gene expression at the transcriptional level.

Table 1
Comparisons between immobilization-based/immobilization-free and/or label-based/label-free nucleic acid-based biosensors.

Signal readout modes	Principle	Key words	Target molecule	Linear range	Limit of detection	Reference
Label-free	intrinsic redox-active properties of DNA bases DNA-gold affinity interactions	immobilization-based aptamer, magnetic beads, PCR immobilization-free, PCR	thrombin	17 fM-2.7 nM	5.4 fM	31
Label-based	electro-active intercalators peroxidase-mimicking DNAzymes redox-active indicators	immobilization-free, G-quadruplex, aptamer immobilization-based, G-quadruplex	cocaine	5–1000 μM	5 μM	32
Label-based	electro-active intercalators peroxidase-mimicking DNAzymes redox-active indicators	immobilization-based, G-quadruplex	thrombin	0.01–50 nM	2 pM	33
Label-based	electro-active intercalators peroxidase-mimicking DNAzymes redox-active indicators	immobilization-free, G-quadruplex	cocaine	1–500 μM	1 μM	34
Label-based	electrochemical molecular beacons	immobilization-based, carminic, aptamer, magnetic nanobeads	thrombin	11.8–141 pM	4.24 pM	35
Label-free	crRNA-based molecular beacons	immobilization-free, aptamer	thrombin VEGF	0.2–3.8 μM 0.2–3.0 μM	88 nM 55 nM	This study

Table 2
Detection of thrombin in 100-fold diluted human serum sample.

Sample	thrombin added (μM)	G-EL sensor for thrombin detection			ELISA for thrombin detection		
		Amount measured (μM)	Recovery (%)	RSD (%)	Amount measured (μM)	Recovery (%)	RSD (%)
1	0.2	0.224	112	4.8	0.187	93.5	2.7
2	1.0	0.893	89.3	5.4	1.078	107.8	1.6
3	1.5	1.672	111.5	3.2	1.432	95.5	3.1
4	2.0	2.348	117.4	7.8	2.113	105.7	1.9
5	3.0	2.788	89.6	6.3	2.879	96.0	3.2

conformational changes.

The aptamer-based sensors in the literatures are usually operated in the micromolar range, restricted by the typical affinity for aptamers towards chemicals [14], while the developed G-EL sensor in this study can take functions in the sub-micromolar range, even has the potential to work in the nanomolar or picomolar range as the detecting mechanism of microbial gene expression is very sensitive to the surrounding environment [41,42]. The approach developed in this study can be used to construct sensors for detecting various chemicals by screening the corresponding aptamers, therefore, this strategy can potentially provide a new set of analytical tools in the field of analytical chemistry.

Author contribution

JW and DMY performed the experiments, XGG and QTS revised the manuscript, LXT and LCD designed the work.

Declaration of competing interest

The authors declare that they have no known competing financial interests or personal relationships that could have appeared to influence the work reported in this paper.

Acknowledgements

This work is financially supported by the National Science Foundation of China (21606026, 21776025), Chongqing Science and Technology Commission (CSTC2013jcyA0348), National Key R& D Program of China (2017YFB0603105), and support by China Scholarship Council (201506050056).

Appendix A. Supplementary data

Supplementary data to this article can be found online at https://doi.org/10.1016/j.aca.2019.11.071.

References

[1] A.D. Ellington, J.W. Szostak, In vitro selection of RNA molecules that bind specific ligands, Nature 346 (1990) 818–822.
[2] C. Tuerk, L. Gold, Systematic evolution of ligands by exponential enrichment: RNA ligands to bacteriophage T4 DNA polymerase, Science 249 (1990) 505–510.
[3] J. Wang, L. Yang, X. Cui, Z. Zhang, L. Dong, N. Guan, A DNA bubble-mediated gene regulation system based on thrombin-bound DNA aptamers, ACS Synth. Biol. 6 (2017) 758–765.
[4] V.J.B. Ruigrok, M. Levisson, M.H.M. Eppink, H. Smidt, J.V.D. Oost, Alternative affinity tools: more attractive than antibodies? Biochem. J. 436 (2011) 1.
[5] S. Jayasena, Aptamers : an emerging class of molecules that rival antibodies in diagnostics, Clin. Chem. 45 (1999) 1628.
[6] Haixiang Yu, Juan Canoura, Bhargav Guntupalli, Xinhui Lou, Yi Xiao, A cooperative-binding split aptamer assay for rapid, specific and ultrasensitive fluorescence detection of cocaine in saliva, Chem. Sci. 8 (2016) 131–141.
[7] T. Hermann, Adaptive recognition by nucleic acid aptamers, Science 287 (2000) 820–825.
[8] J. Liu, Z. Cao, Y. Lu, Functional nucleic acid sensors, Chem. Rev. 109 (2009) 1948.
[9] S. Song, L. Wang, L. Jiang, C. Fan, J. Zhao, Aptamer-based biosensors, Trac. Trends Anal. Chem. 27 (2008) 108–117.
[10] B.S. Ferguson, D.A. Hoggarth, D. Maliniak, K. Ploense, R.J. White, N. Woodward, K. Hsieh, A.J. Bonham, M. Eisenstein, T.E. Kippin, Real-time, aptamer-based tracking of circulating therapeutic agents in living animals, Sci. Transl. Med. 5 (2013) 213ra165.
[11] J. Liu, Y. Lu, Colorimetric sensing of adenosine and cocaine based on a general sensor design involving aptamers and nanoparticles, Angew. Chem. Int. Ed. 45 (2006) 90–94.
[12] W. Mok, Y. Li, Recent progress in nucleic acid aptamer-based biosensors and bioassays, Sensors 8 (2008) 7050–7084.
[13] J. Wang, X. Cui, J. Zhu, L. Tan, L. Dong, A novel photosensitive dual-sensor for simultaneous detection of nucleic acids and small chemical molecules, Biosens. Bioelectron. 127 (2019) 108–117.
[14] Y. Wang, J. Killian, K. Hamasaki, R.R. Rando, RNA molecules that specifically and stoichiometrically bind aminoglycoside antibiotics with high Affinities\\r ? Biochemistry 35 (1996) 12338–12346.
[15] M.N. Stojanovic, P.D. Prada, D.W. Landry, Aptamer-based folding fluorescent sensor for cocaine, J. Am. Chem. Soc. 123 (2001) 4928–4931.
[16] K.A. Yang, M. Barbu, M. Halim, P. Pallavi, B. Kim, D.M. Kolpashchikov, S. Pecic, S. Taylor, T.S. Worgall, M.N. Stojanovic, Recognition and sensing of low-epitope targets via ternary complexes with oligonucleotides and synthetic receptors, Nat. Chem. 6 (2014) 1003–1008.
[17] L.C. Bock, L.C. Griffin, J.A. Latham, E.H. Vermaas, J.J. Toole, Selection of single-stranded DNA molecules that bind and inhibit human thrombin, Nature 355 (1992) 564–566.
[18] D.E. Huizenga, J.W. Szostak, A DNA aptamer that binds adenosine and ATP, Biochemistry 34 (1995) 656–665.
[19] J.H. Lee, M.V. Yigit, D. Mazumdar, Y. Lu, Molecular diagnostic and drug delivery agents based on aptamer-nanomaterial conjugates, Adv. Drug Deliv. Rev. 62 (2010) 592–605.
[20] E.J. Cho, J.-W. Lee, A.D. Ellington, Applications of aptamers as sensors, Annu. Rev. Anal. Chem. 2 (2009) 241–264.
[21] M. Maureen, D.M. C, Challenges and opportunities for small molecule aptamer development, J. Nucleic Acids 2012 (2012) 748913, 2012,(2012-9-17).
[22] M.N. Stojanovic, D.W. Landry, Aptamer-based colorimetric probe for cocaine, J. Am. Chem. Soc. 124 (2002) 9678–9679.
[23] T.R. Cech, J.A. Steitz, The noncoding RNA revolution—trashing old rules to forge new ones, Cell 157 (2014) 77–94.
[24] F. Sven, E. Maja, W. Sebastian, M.r. Mario, S. Peter, Design of artificial riboswitches as biosensors, Sensors 17 (2017) 1990.
[25] A. Serganov, E. Nudler, A decade of riboswitches, Cell 152 (2013) 17–24.
[26] V. Ramakrishnan, Ribosome structure and the mechanism of translation, Cell 108 (2002) 557–572.
[27] G. Storz, J.r. Vogel, K.M. Wassarman, Regulation by small RNAs in bacteria: expanding frontiers, Mol. Cell 43 (2011) 880–891.
[28] M. Krishnamurthy, S.P. Hennelly, T. Dale, S.R. Starkenburg, C.J. Unkefer, Tunable riboregulator switches for post-transcriptional control of gene expression, ACS Synth. Biol. 4 (2015), 150727155643003.
[29] J. Wang, H. Wang, L. Yang, L. Lv, Z. Zhang, B. Ren, L. Dong, N. Li, A novel riboregulator switch system of gene expression for enhanced microbial production of succinic acid, J. Ind. Microbiol. Biotechnol. 45 (2018) 1–17.
[30] M. Zuker, Mfold web server for nucleic acid folding and hybridization prediction, Nucleic Acids Res. 31 (2003) 3406–3415.
[31] B.R. Baker, R.Y. Lai, M.S. Wood, E.H. Doctor, A.J. Heeger, K.W. Plaxco, An electronic, aptamer-based small-molecule sensor for the rapid, label-free detection of cocaine in adulterated samples and biological fluids, J. Am. Chem. Soc. 128 (2006) 3138.
[32] P.C. Anderson, Identification of a 14mer RNA that recognizes and binds flavin mononucleotide with high affinity, Nucleic Acids Res. 33 (2005) 6992–6999.
[33] K. Wang, D. Fan, Y. Liu, E. Wang, Highly sensitive and specific colorimetric detection of cancer cells via dual-aptamer target binding strategy, Biosens. Bioelectron. 73 (2015) 1–6.
[34] S. Balamurugan, A. Obubuafo, R.L. Mccarley, S.A. Soper, D.A. Spivak, Effect of linker structure on surface density of aptamer monolayers and their corresponding protein binding efficiency, Anal. Chem. 80 (2008) 9630–9634.
[35] Y. Xiang, M. Xie, R. Bash, J. Julian, L. Chen, J. Wang, Ultrasensitive label-free aptamer-based electronic detection, Angew. Chem. Int. Ed. 46 (2010) 9054–9056.

[36] F.T. Zhang, J. Nie, D.-W. Zhang, J.-T. Chen, Y.-L. Zhou, X.-X. Zhang, Methylene blue as a G-quadruplex binding probe for label-free homogeneous electrochemical biosensing, Anal. Chem. 86 (2014) 9489–9495.
[37] Y. Yuan, X. Gou, R. Yuan, Y. Chai, Y. Zhuo, L. Mao, X. Gan, Electrochemical aptasensor based on the dual-amplification of G-quadruplex horseradish peroxidase-mimicking DNAzyme and blocking reagent-horseradish peroxidase, Biosens. Bioelectron. 26 (2011) 4236–4240.
[38] D.-W. Zhang, J. Nie, F.-T. Zhang, L. Xu, Y.-L. Zhou, X.-X. Zhang, Novel homogeneous label-free electrochemical aptasensor based on functional DNA hairpin for target detection, Anal. Chem. 85 (2013) 9378–9382.
[39] S.D. Bell, S.P. Jackson, The role of transcription factor B in transcription initiation and promoter clearance in the archaeon Sulfolobus acidocaldarius, J. Biol. Chem. 275 (2000) 12934–12940.
[40] L.V. Crawford, C.N. Cole, A.E. Smith, E. Paucha, P. Tegtmeyer, K. Rundell, P. Berg, Organization and expression of early genes of simian virus 40, in: Proceedings of the National Academy of Sciences of the United States of America, vol. 75, 1978, pp. 117–121.
[41] J. Wang, D.D. Qin, B.Y. Zhang, Q. Li, S. Li, X.H. Zhou, L.C. Dong, D. Wang, Fine-tuning ofecaAandpepcgene expression increases succinic acid production in Escherichia coli, Appl. Microbiol. Biotechnol. 99 (2015) 8575–8586.
[42] J. Wang, X. Cui, L. Yang, Z. Zhang, L. Lv, H. Wang, Z. Zhao, N. Guan, L. Dong, R. Chen, A real-time control system of gene expression using ligand-bound nucleic acid aptamer for metabolic engineering, Metab. Eng. 42 (2017) 85–97.

Please cite this article as: J. Wang et al., A novel RNA aptamer-modified riboswitch as chemical sensor, Analytica Chimica Acta, https://doi.org/10.1016/j.aca.2019.11.071